

## Computational Fluid Dynamics Simulation of Bubble Column Reactor Hydrodynamics

R. RAHIMI, M.A. SALEHI\* and K. NANDAKUMAR†

*Department of Chemical Engineering  
Sistan and Baluchestan University*

*Shahid NIKBAKHT Faculty of Engineering, Daneshgah A.V., Zahedan, Iran  
E-mail: salehi@hamoon.usb.ac.ir*

In this research, hydrodynamic behaviour of a bubble column reactor was determined. In previous works, the prediction of gas holdup is not accurately covered. For that reason, the turbulence in liquid phase is modelled by standard k- $\epsilon$  model. In addition, local axial velocity, velocity distribution and local gas hold-up were calculated by Fluent 6.0.3, which is a commercial software. The results have been compared with experimental data, which show quite a good agreement.

**Key Words:** Computational fluid dynamics, Bubble column reactor, Hydrodynamic.

### INTRODUCTION

A bubble column reactor is a multiphase flow reactor in which reactant gas is bubbled through a liquid solution. Bubble column reactors may be operated in a batch or continuous mode. They are known as excellent reactors for processes, which require large interfacial area for gas-liquid mass transfer and efficient mixing for reacting species, for example, in bubble column fermentors. A better knowledge of the local hydrodynamics to increase the predictability of the reactor design and to improve the efficiency of the processes appears currently necessary. The use of numerical modelling, *i.e.*, computational fluid dynamics (CFD) should be able to improve this knowledge by providing a complete description of the local hydrodynamics if an adequate model is used.

Bubble column reactors are widely used as gas liquid contactors in industrial fermentation, hydrogenation and other chemical operations because of their simple construction and ease of maintenance. Bubble column reactors combine efficient gas transfer and mixing with low shear forces. The behaviour of these reactors is determined by their hydrodynamic properties. The complex flow and mixing behaviour found in bubble column reactors are often described by means of local parameters such as gas holdup and axial liquid velocity. There is currently strong effort in academic institutions and industry to enable the use of computa-

---

†Department of Chemical and Material Engineering, University of Alberta, Edmonton, Alberta, Canada, T6G 2G6.

tional fluid dynamics (CFD) for the design, scale up and optimum operation of bubble column reactors. The simulation of bubbly flow is still not fully mastered mainly due to its complexity and the manifold interacting phenomena. The movement of the bubbles dominates the bubble column reactor hydrodynamics and the two-dimensional flow structures in the liquid phase that continuously change size and position. Most of the transient CFD studies of the last decade focussed on flat bubble column reactors with a rectangular cross-section because they have a less complex flow structure. They proved to be a useful tool for numerical model development and validation. Many models have been proposed to analyze and predict liquid axial velocity. Migauchi and Shyu<sup>1</sup> and Joshi and Sharma<sup>2</sup> predicted liquid velocity in relation to the local gas holdup. However, the local gas holdup must be obtained from experimental data for both of these models. Zehner<sup>3</sup> introduced a friction factor for liquid velocity prediction, but the value assigned by him to this parameter is not easy to justify.

### Theory

**Hydrodynamic:** The basic hydrodynamic model used for the simulations is described in detail in Pflieger *et al.*<sup>4</sup> In this study, based on this paper and the commercial CFD software package (Fluent 6.0.3), the hydrodynamics of bubble column was investigated. The code is based on the finite volume technique. A two-phase model or Eulerian-Eulerian description is applied for the two-phase gas liquid flow. The basics of the two-phase model can be found in Ishii<sup>5</sup>.

**Basic model equations:** The basic equation set consists of the continuity and momentum equations for  $N_p$  phases. The first one is expressed by

$$\frac{\partial}{\partial t} (\rho_\alpha r_\alpha) + \frac{\partial}{\partial x_i} (\rho_\alpha r_\alpha u_{\alpha, i}) = \sum_{\beta=1}^{N_p} (\dot{m}_{\alpha\beta} - \dot{m}_{\beta\alpha} + r_\alpha S_\alpha) \quad (1)$$

The right hand side of the continuity equation describes mass transfer from phase  $\alpha$  to  $\beta$  as well as *vice-versa* and includes additional source terms. In this work, mass transfer and source terms were neglected. Therefore, Eq. (1) simplifies to

$$\frac{\partial}{\partial t} (\rho_\alpha r_\alpha) + \frac{\partial}{\partial x_i} (\rho_\alpha r_\alpha u_{\alpha, i}) = 0 \quad (2)$$

where  $r_\alpha$  represents the volume fraction of phase  $\alpha$ . The sum over all  $N_p$  phases satisfies the relation:

$$\sum_{i=1}^{N_p} r_i = 1 \quad (3)$$

In analogy with mass conservation the momentum conservation for multiphase flows is described by the Navier-Stokes equations expanded by the phase volume fraction  $r_\alpha$  and the interphase transfer term  $M_{\alpha, i}$ :

$$\frac{\partial}{\partial t} (\rho_\alpha r_\alpha u_{\alpha, i}) + \frac{\partial}{\partial x_j} (\rho_\alpha r_\alpha u_{\alpha, i} u_{\alpha, j}) = -r_\alpha \frac{\partial p}{\partial x_i} + \frac{\partial}{\partial x_i} r_\alpha \mu_\alpha \left( \frac{\partial u_{\alpha i}}{\partial x_j} + \frac{\partial u_{\alpha j}}{\partial x_i} \right) + \rho_\alpha r_\alpha g_i + M_{\alpha, i} \quad (4)$$

The terms on the right hand side describe all forces acting on a fluid element of phase  $\alpha$  in the control volume. These are the overall pressure gradient, the viscous stresses and the gravitational force and interphase momentum forces combined in  $M_{\alpha, i}$ . Only the drag force is included up to now in our model, which is based on Weber *et al.*<sup>6</sup>

$$M_{\alpha, i} = \frac{3}{4} C_d r_{\beta} \rho_{\alpha} \frac{1}{d_b} |u_{\beta} - u_{\alpha}| (u_{\beta} - u_{\alpha})$$

The drag coefficient ( $C_d = 0.44$ ) and bubble diameter ( $d_b = 4$  mm) is set constant in the simulations to define a fixed slip velocity between bubbles and surrounding liquid of around  $20 \text{ cm s}^{-1}$ . The use of a more complex drag model did not result in better agreements. Due to the fact that simulation results are not sensitive with respect to a fixed slip velocity in our regime, it is reasonable to use this model assumption. Coalescence and bubble breakup are not considered in this model. The impact of these phenomena is negligible for our test case configuration and conditions.

**Turbulence equations:** Turbulence is taken into consideration for the continuous phase. The dispersed gas phase is modelled laminar but influences the turbulence in the continuous phase by a bubble-induced turbulence model. In the well known single-phase standard  $k$ - $\epsilon$  turbulence model the turbulence phenomena is a continuous phase of the gas-liquid flow. Its transport equations for the turbulent kinetic energy  $k$  and turbulent dissipation rate  $\epsilon$  are:

$$\begin{aligned} \frac{\partial}{\partial t} (r_{\alpha} \rho_{\alpha} k_{\alpha}) + \frac{\partial}{\partial x_i} (r_{\alpha} \rho_{\alpha} u_{\alpha, i} k_{\alpha}) - \frac{\partial}{\partial x_i} \left( r_{\alpha} \left( \mu_{\alpha, \text{lam}} \frac{\mu_{\alpha, \text{tur}}}{\sigma_k} \right) \frac{\partial k_{\alpha}}{\partial x_i} \right) \\ = r_{\alpha} (G_{\alpha} - \rho_{\alpha} \epsilon_{\alpha}) + S_{\alpha, k} \end{aligned} \quad (6)$$

$$\begin{aligned} \frac{\partial}{\partial t} (r_{\alpha} \rho_{\alpha} \epsilon_{\alpha}) + \frac{\partial}{\partial x_i} (r_{\alpha} \rho_{\alpha} u_{\alpha, i} \epsilon_{\alpha}) - \frac{\partial}{\partial x_i} \left( r_{\alpha} \left( \mu_{\alpha, \text{lam}} \frac{\mu_{\alpha, \text{tur}}}{\sigma_{\epsilon}} \right) \frac{\partial \epsilon_{\alpha}}{\partial x_i} \right) \\ = r_{\alpha} \frac{\epsilon_{\alpha}}{k_{\alpha}} (C_{\epsilon_1} G_{\alpha} - C_{\epsilon_2} \rho_{\alpha} \epsilon_{\alpha}) + S_{\alpha, \epsilon} \end{aligned} \quad (7)$$

The standard model is taken without any further modifications. The source terms  $S_{\alpha, \epsilon}$  on the right-hand side of the equations are not considered in the mean of interphase turbulence exchange. The effective viscosity of phase  $\alpha$  in Eq. (7) is combined by

$$\mu_{\alpha, \text{eff}} = \mu_{\alpha, \text{lam}} + \frac{\mu_{\alpha, \text{tur}}}{\sigma_k} \quad (8)$$

Using the standard  $k$ - $\epsilon$  model the turbulent viscosity of the continuous phase is calculated by:

$$\mu_{c, \text{tur}} = C_{\mu} \rho_c \frac{k_c^2}{\epsilon_c} \quad (9)$$

One of the main objectives of this investigation is evaluation of bubble-induced turbulence in gas-liquid flow which seems to have an important impact on the correctness of simulation results<sup>7</sup>. A direct coupling of turbulence equations *via* an inter-phase exchange term similar to the one of the momentum equation is not possible due to the missing set of equations for turbulence in the gas flow. Nevertheless, the influence of bubbles on turbulence can be captured by implementing additional production terms in  $k$ - $\epsilon$  equations. The term  $G_\alpha$  is production of turbulence by the local shear forces in the continuous phase. It is imaginable that wakes behind rising bubbles cause additional stresses, which influence the turbulence intensity. The advanced approach is defined as

$$G_\alpha = \mu_{\alpha, \text{eff}}(\nabla u_\alpha + \nabla u_\alpha^T) : \nabla u_\alpha + G_{\alpha, \text{BIT}} \quad (10)$$

in which the velocity gradients of the first term model the shear-induced production. The energy input of the bubble wakes results from the forces acting between a gas bubble and the surrounding liquid and the local slip velocity.

Since only the drag force is acting in the recent modelling approach the bubble-induced turbulence term is proportional to the inter-phase exchange term  $M_{\alpha, i}$  and is represented by eqn. (5). The constants  $C_{k/\epsilon}$  correspond either to the  $k$  or  $\epsilon$  equation and are combined with standard  $k$ - $\epsilon$  constants. Here,  $C_k, C_{\epsilon_1}$  is equal to 1.44 and  $C_\epsilon, C_{\epsilon_2}$  is set to 1.92 and  $k$ - $\epsilon$  are assumed constant. Also, similar approaches for bubble-induced turbulence are published by Kataoka and Serizawa<sup>8</sup> and Lopez de Bertodano<sup>9</sup>.

**CFD simulation setup:** The first step in developing the computer simulation was to create a 3-D model of the bubble column reactor. For this reason, Gambit Fluent's preprocessor was used, that permits both geometry creation and meshing. The geometry of the column, which shows in Fig. 3 that it was basically a vertical cylinder with a velocity inlet at the bottom and an outflow at the top, was simple to create. After that the Gambit software generated the mesh. The next step was imposed by the boundary conditions for the problem. The bubble column is divided into grids of different resolutions to evaluate grid (in)dependence. The grids consist of 4,175 to 78,900 cells. In this work, 14,500 cells represent the standard grid. The geometry is represented in three dimensions through Cartesian coordinates. The circular cross-section is divided into a central square with  $3 \times 3$  cells plus 4 rim zones with  $3 \times 7$  cells for the standard grid. The latter ones fill one-quarter of a circle between the circular wall boundary and the centre square. The axial direction is split up into 80 cells with grading to the gas sparger modelled by an inlet boundary condition. The standard grid subdivision is chosen after examining mesh tests in the tension between the exactness of simulation and requirements of CPU time. The solution of the equation system is carried out using the SIMPLEC procedure. The application of higher order differencing schemes like total variation diminishing is necessary to obtain accurate solution which is well known for Eulerian-Eulerian multiphase models<sup>10</sup>.

The computational effort is still very high for two-phase transient simulations. The transient solution proceeds with a time stepping of 0.1 of a second over time ranges of up to 1700 s respective *ca.* 25 min real time. Such long-time-averaging procedures are necessary to obtain a well established mean value<sup>4, 11</sup>. The necessity of long averaging times is also observed for the LDA measurements where measuring periods of up to 1 h are required depending on the data rate. The overall calculation of the 5 min real time increment needs roughly 300 min of CPU time on a workstation with parallel Dual 2.46 (GHz) processor. Therefore, simulations with a long time averaging procedure of 1,700 s need calculation times in the order of 36 h for a (relatively coarse) standard grid. The finest grids need roughly 11 days of calculation time that is not acceptable for model investigations or for the detailed influence evaluation of operating parameters. For these efficiency reasons most of the simulations are carried out on the standard grid with fixed time increments which seems to be a good compromise between efficiency and quality of results as shown in results.

## RESULTS AND DISCUSSION

To get a better understanding of gas-liquid flow structure, the gas volume fraction profiles obtained by Spicka *et al.*<sup>12</sup> with standard imaging technique (IP) and local axial velocity obtained by D. Broder *et al.*<sup>13</sup> with particle image velocimetry (PIV) is applied. The experimental results compare with the numerical simulation results. Two main simulated evolutions of variables are investigated. They consist in the evolution of average gas volume fraction and local axial velocity. The gas volume fraction,  $e_G$ , or gas holdup, is a fundamental quantity in the description and analysis of multiphase flow since it affects the flow regime, pressure drop, phase velocity distribution and heat and mass transfer characteristics. Generally, its distribution is influenced mainly by the gas and liquid flow rates, but also by the fluid properties and the column geometry. The evolution of average gas holdup with superficial gas velocity is compared to the experimental values (Fig. 2) and shows a good prediction of the experimental data. Figs. 1, 3 show the evolution of local axial velocity with radial distance and average gas holdup under difference pressure at constant superficial gas velocity (0.2 m/s) while, in this case, it can be seen that there is not a completely good agreement between the experimental and simulated values that are discussed in the conclusion. Further work showed that an excellent agreement can be seen between the CFD prediction and the experimental data for the pressure drop with this model applied<sup>14</sup>. Figs. 5, 6 show the distribution of velocity-by-velocity magnitude for a three-dimensional bubble column in Reynolds 10000 and two-dimensional bubble column in Reynolds 2500. Fig. 7 shows the distribution of gas volume fraction contour or gas holdup in Reynolds 2500. Thus, the CFD simulation enables the estimation of average gas holdup and pressure drop with these models. It can be seen with the difference models that computational

fluid dynamics can be easily estimated and predicted for the other important parameters.

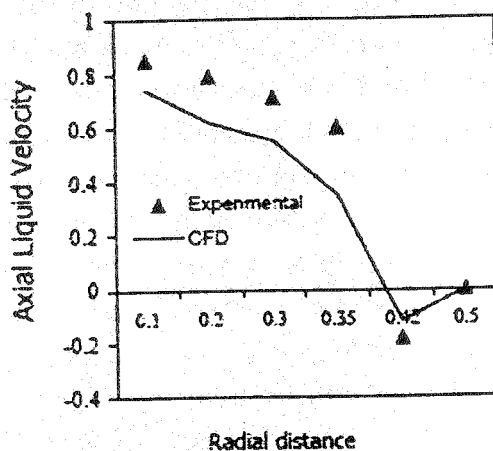


Fig. 1. Axial liquid velocity (m/s) as a function of radial distance (m) in bubble column reactor compared between experimental values and calculated by CFD

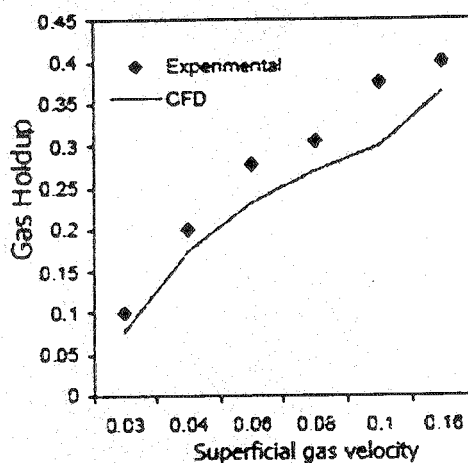


Fig. 2. Gas holdup as a function of superficial gas velocity (m/s) in bubble column reactor compared between experimental values and calculated by CFD

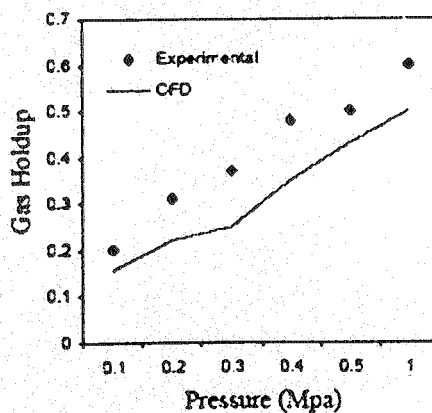


Fig. 3. Gas holdup as a function of difference pressure at ( $u_g = 0.2$  m/s) in bubble column reactor compared between experimental values and calculated by CFD

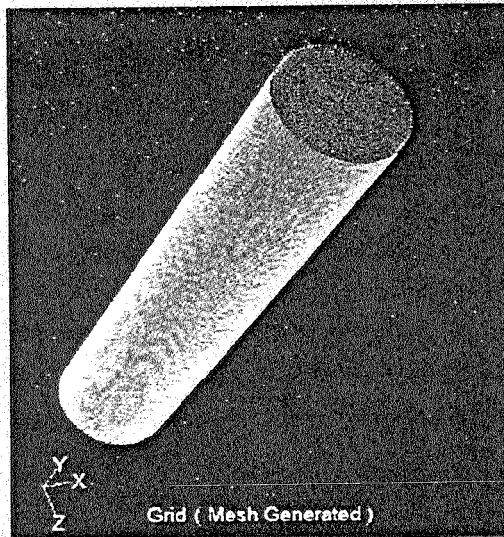


Fig. 4. Geometry and mesh generated of cylindrical bubble column

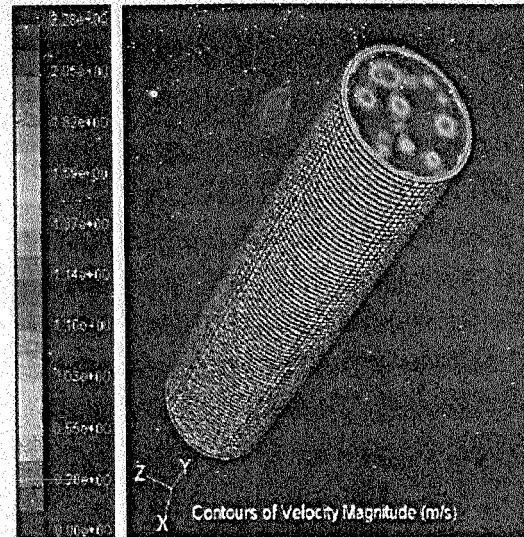


Fig. 5. Contour of velocity magnitude of air shown in Reynolds-10000

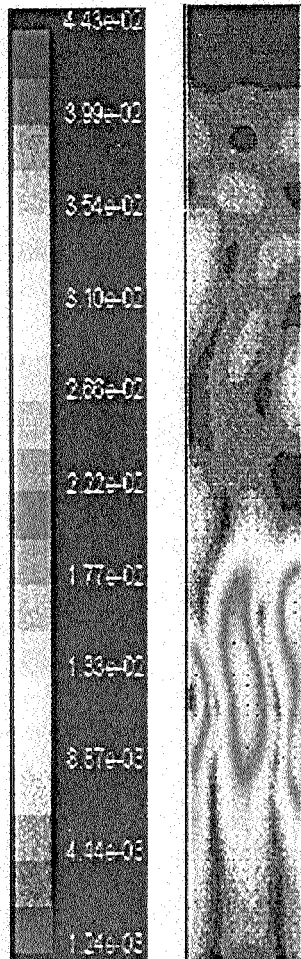


Fig. 6. Contour of velocity magnitude of air obtained in  $t = 4$  s, Reynolds = 2500

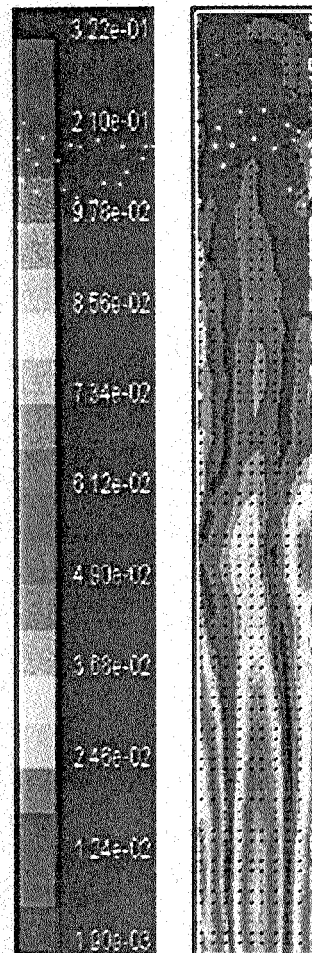


Fig. 7. Contour of volume fraction of air (holdup) obtained in  $t = 4$  s, Reynolds = 2500



## Conclusion

A good agreement has been shown between the experimental measurements and the CFD prediction. Also the selection of models is very important, for example, with the k- $\epsilon$  model that was selected for the kind of turbulence, it can be seen that while this model for volume fraction of air or gas holdup and pressure drop was an excellent model, but for axial liquid velocity, it was not a completely good model. Thus, the present trend has been to use the same turbulence parameters as those for single-phase flows. A systematic knowledge is needed for understanding the physical significance of the turbulence parameters in the presence of interface forces and interface energy transfer. For k- $\epsilon$  model, the effect of mesh size needs to be investigated further. Finer mesh size will bring out further details in the flow structure. In addition, flow near the wall needs simulation for understanding the transport phenomena, which is of great interest. The progress in CFD will continue with the development in computers; now there is need to simulate the relation between flow patterns and design.

## REFERENCES

1. G. Hilmer, L. Weismantel and H. Hofmann, *Chem. Engg. Sci.*, **49**, 837 (1994).
2. R. Krishna, J.M. Vanbaten and M.I. Urseanu, *Chem. Engg. Sci.*, **55**, 3275 (2000).
3. V.V. Ranade, *Amer. Inst. Chem. Eng. Symp. Ser.*, **89**, 6171 (1992).
4. ———, *Chem. Engg. Res. Des.*, **75**, 14 (1997).
5. A. Sokolichin and G. Eigenberger, *Chem. Engg. Sci.*, **49**, 5735 (1994).
6. J.B. Joshi, *Chem. Engg. Sci.*, **56**, 5893 (2001).
7. A. Lapin and A. Lubbert, *Inst. Chem. Eng. Symp. Ser.*, **136**, 365 (1994).
8. H.A. Jakobsen, *Chem. Engg. Sci.*, **56**, 1049 (1993).
9. J. Sanyal, S. Vasquez *et al.*, *Chem. Engg. Sci.*, **54**, 5071 (1999).

(Received: 7 October 2004; Accepted: 5 September 2005)

AJC-4371

## 7<sup>th</sup> METHODS AND APPLICATIONS OF RADIOANALYTICAL CHEMISTRY

3-7 APRIL 2006

KONA, HAWAII, USA

*Contact:*

Samuel E. Glover

National Institute of Occupational Safety and Health

4676 Columbia Pkw, MS C45

Cincinnati, OH 45221, USA

E-mail: [sglover@cdc.gov](mailto:sglover@cdc.gov)

Web: [www.min.uc.edu/nuclear/marc/](http://www.min.uc.edu/nuclear/marc/)